Supplementary Information

Residue-based Program of a β-Peptoid Twisted Strand Shape via a Cyclopentane Constraint

Jungyeon Kim,[a] Hiroka Kobayashi,[a] Marin Yokomine,[a] Yota Shiratori,[b] Takumi Ueda,[c] Koh Takeuchi,[c] Koji Umezawa,[d,e] Daisuke Kuroda,[a,b] Kouhei Tsumoto,[a,b,f] Jumpei Morimoto,*[a] and Shinsuke Sando*[a,b]

a. Department of Chemistry and Biotechnology, Graduate School of Engineering, The University of Tokyo, 7-3-1 Hongo, Bunkyo-ku, Tokyo 113-8656, Japan.

b. Department of Bioengineering, Graduate School of Engineering, The University of Tokyo, 7-3-1 Hongo, Bunkyo-ku, Tokyo 113-8656, Japan.

c. Graduate School of Pharmaceutical Sciences, The University of Tokyo, 7-3-1 Hongo, Bunkyo-ku, Tokyo, 113-0033 Japan

d. Department of Biomedical Engineering, Graduate School of Science and Technology, Shinshu University, Minamiminowa, Nagano 399-4598, Japan

e. Institute for Biomedical Sciences, Interdisciplinary Cluster for Cutting Edge Research, Shinshu University, Matsumoto, Nagano 390-8621, Japan

f. Institute of Medical Science, The University of Tokyo, 4-6-1 Shirokanedai, Minato-ku, Tokyo 108-8639, Japan.

Table of Contents

Materials and Methods

Abbreviations for chemical compounds. ACPC, 2-aminocyclopentanecarboxylic acid; DCM, dichloromethane; DMSO, dimethylsulfoxide; MeCN, acetonitrile; DIPEA, *N,N*-diisopropylethylamine; DMF, *N,N*-dimethylformamide; TFA, trifluoroacetic acid; Fmoc, 9-fluorenylmethyloxycarbonyl; COMU, (1-cyano-2-ethoxy-2-oxoethylideneaminooxy)dimethylamino-morpholino-carbenium hexafluorophosphate; HFIP, 1,1,1,3,3,3-hexafluoro-2-propanol.

General remarks. All the chemicals were purchased from commercial suppliers and used without further purifications. Preparative HPLC was performed on a Prominence HPLC system (Shimadzu) with a 5C18-AR-II column (Nacalai tesque, 10 mm I.D.×150 mm, 34355-91). Ultra performance liquid chromatography (UPLC) was performed on a ACQUITYUPLC H-Class (Waters) using InertSustain AQ-C18 (GL Science, 2.1 I.D. x 50 mm). Elution was monitored with absorbance at 220 nm. HRMS data was obtained using micrOTOF II (Bruker Daltonics). All the molecular mechanics calculations were performed with Avogadro: an open-source molecular builder and visualization tool. Version 1.2.0.[1] http://avogadro.cc/. All the DFT calculations were carried out with the Gaussian16 package at the B3LYP/6-31G* level.[2]

Synthesis of Fmoc-(*1R,2R*)ACPC-OH. The compound was synthesized according to the previous report.[3] 6.46 g (18.4 mmol) of Fmoc-(*1R,2R*)ACPC-OH was obtained as a white solid from 23.0 mL (159 mmol) of ethyl 2-oxocyclopentanecarboxylate (12%). ^{1}H NMR (DMSO-d_6, 400 MHz): δ 12.33–11.87 (br s, 1H), 7.89 (d, 2H, J = 7.3 Hz), 7.75–7.60 (m, 2H), 7.52–7.28 (m, 5H), 4.39–4.14 (m, 3H), 4.08–3.96 (m, 1H), 2.59 (q, 1H), 2.02–1.20 (m, 6H). ^{13}C NMR (DMSO-d_6, 100 MHz): δ 175.9, 155.5, 144.0, 143.9, 140.7, 127.6, 127.1, 125.1, 120.1, 65.2, 55.4, 49.3, 46.7, 32.6, 28.5, 22.9. $[\alpha]^{23}_D$ = –33.9 (*c* 1.21, methanol). HRMS (ESI-TOF MS) *m/z*: [M + Na]$^+$ Calcd for $C_{21}H_{21}NO_4Na^+$ 374.1363; Found 374.1358.

Generation of Ramachandran-type plot of acetyl-*N*-methyl-(*1R,2R*)ACPC dimethylamide (Me1). The initial conformation of **Me1** was set as described in the manuscript. The structure was minimized by molecular mechanics calculations before DFT calculations. Conformers of **Me1** were systematically generated by combinatorically fixing φ and ψ at every 15° from –180° to 180° and each conformer was optimized *in vacuo*. ω angle was fixed at either 0° or 180° throughout the calculations. The dihedral angle θ was allowed to freely move during the optimization.

Evaluation of the relative stability of conformer 1 over conformer 2 of acetyl-*N*-ethyl-(*1R,2R*)ACPC dimethylamide (Et1) by DFT calculations. An ethyl group was introduced to the **conformer 1** and **conformer 2** of **Me1** by substituting the methyl group on the nitrogen of the ACPC residue to generate the initial conformation of **Et1**. To investigate an appropriate orientation of the *N*-substituent, χ_N scan was first conducted for both the **conformer 1** and **conformer 2** (**Fig. S1a** and **b**). The χ_N angle that defines the direction of the ethyl group was initially set to –180° and the χ_N angle was rotated by 15° from –180° to 180°. Each conformer was optimized *in vacuo*. During the calculations, ω angle of acetylamide, and φ, θ and ψ angles were fixed at the values in the initial conformation. Based on the result, χ_N angle was

set to the value that gave the lowest energy for each conformer, and the conformer was geometry optimized *in vacuo* and the relative energy of the optimized conformations shown in **Table 1** was calculated.

Evaluation of the relative stability of conformer 1 over conformer 2 of acetyl-*N*-propyl-(*1R,2R*)ACPC dimethyla-mide (Pr1), acetyl-*N*-isobutyl-(*1R,2R*)ACPC dimethylamide (Ib1) and acetyl-*N*-neopentyl-(*1R,2R*)ACPC dime-thylamide (Np1) by DFT calculations. A propyl, isobutyl, and neopentyl group was introduced to the **conformer 1** and **conformer 2** of **Et1** by substituting the ethyl group on the nitrogen to generate the initial conformation of **Pr1**, **Ib1** and **Np1**, respectively. To investigate an appropriate orientation of the *N*-substituent, χ_{N2} scan was first conducted for both the **conformer 1** and **conformer 2**. The χ_{N2} angles were initially set to $-180°$ and the χ_{N2} angle was rotated by $15°$ from $-180°$ to $180°$. Each conformer was optimized *in vacuo*. During the calculations, ω angle of acetylamide, and φ, θ, ψ and χ_N angles were fixed at the values in the initial conformation. Based on the result (data not shown), χ_{N2} angle was set, and the conformer was geometry optimized *in vacuo* and the relative energy of the optimized conformations was calcu-lated.

Optimization of the structure of Ib2, Ib3 and Ib4 *in vacuo* by DFT calculations. First, the structures of **Ib2**, **Ib3** and **Ib4** were prepared by connecting the structure of **conformer 1** or **conformer 2** of **Ib1** that was optimized by DFT cal-culations. The generated structure was energy-minimized with molecular mechanics calculations using UFF as the force field. The energy-minimized structures were geometry optimized *in vacuo*.

Synthesis of acetyl-*N*-isobutyl-(*1R,2R*)ACPC tetramer dimethylamide (Ib4). 60 mg of Cl-Trt(2-Cl) resin (1.32 mmol/g, 79 μmol) was treated with DCM (anhydrous) solution of Fmoc-(*1R,2R*)ACPC-OH (1.2 equiv, 0.1 M) and DI-PEA (2.4 equiv, 0.2 M) with continuous shaking for 2 h. After removing the solution, the resin was washed with DCM three times and 85/10/5 = DCM/methanol/DIPEA once. The resin was incubated with 85/10/5 = DCM/methanol/DIPEA for 15 min and washed with DCM and DMF three times each. The loading amount of the first amino acid was quantified by measuring UV absorption of the deprotected Fmoc group from a fraction of the resin (62 μmol). The resin was treated with 20% piperidine/DMF (3 min and 12 min) to remove the Fmoc protecting group and washed with DMF three times. After deprotecting the Fmoc group, the resin was incubated with isobutyraldehyde (20 equiv, 1 M) solution in DMF for 1 h. The aldehyde solution was removed and the resin was quickly washed with DMF and DCM. A freshly prepared sus-pension of NaBH$_4$ (10 equiv, 0.5 M) in 3/1 DCM/methanol was added to the resin and the syringe was continuously shaken for 30 min. The reaction was conducted with the lid open to release evolving gas. The resin was washed with methanol five times then with DMF and DCM three times each. The resin was washed with 1/1 MeCN/DMF three times. The resin was treated with Fmoc-(1*R*,2*R*)ACPC-OH (3 equiv, 0.2 M), COMU (3 equiv, 0.2 M) and DIPEA (6 equiv, 0.4 M) in 1/1 MeCN/DMF (anhydrous) for 3 h at 60 °C. After the reaction, the resin was washed with DMF three times. Procedures for Fmoc group deprotection, reductive amination and coupling reaction were repeated to produce a β-peptoid tetramer on resin. Then the resin was washed with 1/1 MeCN/DMF three times. The resin was treated with acetic acid (4 equiv, 0.2 M), COMU (4 equiv, 0.2 M) and DIPEA (8 equiv, 0.4 M) in 1/1 MeCN/DMF (anhydrous) for 3 h at 60 °C. After the reaction, the resin was washed with DMF and DCM three times each. The compound was cleaved

from the resin by treating the resin with 1 mL of 30% HFIP/DCM (v/v) for 30 min three times. The resin was washed with DCM and methanol three times each, and the solutions were combined to the HFIP/DCM solution. The solution was concentrated, and the crude product was dissolved in MeCN and water and purified with a reversed phase column on HPLC using MeCN and water containing 0.1% TFA as mobile phases. Yield was 10.6 mg (14.6 μmol, 24% compared with the loading amount of the first amino acid). The purified β-peptoid oligomer (1 equiv) and COMU (1.5 equiv, final conc. 0.03 M) were dissolved in dry MeCN, and 2 M dimethylamine in tetrahydrofuran (2 equiv, final conc. 0.04 M) and DIPEA (2 equiv, final conc. 0.04 M) were added. The mixture was stirred at 60 °C for 7.5 h. After stirring, the solution was concentrated, and dissolved in MeCN and water. The compound was purified with a reversed phase column on HPLC using MeCN and water containing 0.1% TFA as mobile phases. The yield was 5.5 mg (7.3 μmol, 50%). The purified product was analyzed on a reversed phase column by UPLC. HRMS (ESI-TOF MS) m/z: $[M + H]^+$ Calcd for $C_{44}H_{78}N_5O_5^+$ 756.5997; Found 756.5968.

Crystallization. 14.0 mg of **Ib4** was dissolved in a mixture of MeCN 25 μL and water 10 μL. Colorless block-shaped crystals were obtained by slow evaporation of the solvent at room temperature.

X-ray crystallography. A single crystal was mounted with mineral oil on a loop-type mount and set on VariMax Dual (Rigaku). The X-ray diffraction data was measured at –180 °C using Cu K$_\alpha$. Data was processed using the Olex2 software (Rigaku). The structure was solved by a direct method using SHELXT7 and refined using SHELXL. The non-hydrogen atoms were refined anisotropically. Hydrogen atoms were placed on ideal positions.

Synthesis of acetyl-*N*-isobutyl-(*1R,2R*)ACPC dimer dimethylamide (Ib2). Ib2 was synthesized in a similar manner with **Ib4**. 150 mg of Cl-Trt(2-Cl) resin (1.32 mmol/g, 198 μmol) was used for the synthesis. After loading Fmoc-(*1R,2R*)ACPC-OH on the resin, the loading amount was determined to be 178 μmol. After oligomer synthesis, cleavage from resin, C-terminal dimethylamidation, and HPLC purification, 15.5 mg of **Ib2** was obtained (21% compared with the loading amount of the first amino acid). The purified product was analyzed on a reversed phase column by HPLC. HRMS (ESI-TOF MS) m/z: $[M + H]^+$ Calcd for $C_{24}H_{44}N_3O_3^+$ 422.3377; Found 422.3374.

NMR spectroscopic studies. NMR spectra of **Ib2** were recorded in CDCl$_3$ on a Bruker Avance 800 spectrometer equipped with a cryogenic probe. HMBC spectrum was recorded with x points of 4,096, y points of 4,096, relaxation delay of 1.5 s and receiver gain of 203. COSY spectrum was recorded with relaxation delay of 1.5 s and receiver gain of 57. TOCSY spectrum was recorded with relaxation delay of 1.5 s and receiver gain of 203. The 2D gradient-selected F1-PSYCHE-EASY-ROESY spectrum was recorded using the previously reported pulse program and parameters,[4] with the carrier frequency offset of 3.0 ppm, spectrum width of 6.8 ppm, relaxation delay of 1.5 s, mixing time of 250 ms, and receiver gain of 203. The 2D EASY-ROESY spectrum was recorded using the previously reported pulse program and parameters,[5] with the carrier frequency offset of 4.5 ppm, spectrum width of 9 ppm, relaxation delay of 1.5 s, mixing time of 250 ms, and receiver gain of 64. Chemical shifts of ^{1}H NMR, COSY, HMBC, HSQC and ROESY spectra are reported in p.p.m relative to 3-(trimethysilyl)-1-propanesulfonic acid sodium salt as an external standard. Each peak in

the ^{1}H NMR spectrum was assigned using HMBC, COSY and TOCSY spectra. First, backbone α- and β-protons were sequentially assigned from their intra-residual and inter-residual cross peaks with the carbonyl carbon in the HMBC spectrum. Second, backbone γ- and ε-protons were assigned from their cross peaks with the neighboring β- and α-protons, respectively, in the COSY spectrum. Third, backbone δ-protons were assigned from their cross peaks with the other intra-residual backbone protons in the TOCSY spectrum. Fourth, α-protons on the *N*-substituents were assigned from their inter-residual cross peaks with the carbonyl carbon in HMBC spectrum. Fifth, β- and γ-protons on the *N*-substituents were assigned from their cross peaks with their neighboring protons in the COSY spectrum. The carbonyl carbons in the HMBC spectrum were assigned during the assignment of α- and β-protons described above. The carbons other than carbonyl carbons were assigned using the HSQC spectrum.

Optimization of the structure of Ib2 in chloroform by DFT calculations. First, the **Ib2** structure was prepared by truncating the crystal structure of **Ib4**. The C-terminal two residues were removed from the **Ib4** structure, and the C-terminal structure was converted to dimethylamide. The generated structure was energy-minimized with molecular mechanics calculations using GAFF as the force field. The energy-minimized structure was geometry optimized *in vacuo*.

Molecular dynamics (MD) simulations of Ib4. MD simulations of the **Ib4** in chloroform were performed using AMBER20 with the following force fields.[6] The crystal structure of **Ib4** was used for DFT calculation (B3LYP/6-31G(d,p)) to assign the partial atomic charges. The DFT calculation was done by GAMESS 2019 R2.[7] The partial charges were assigned with RESP method by antechamber in AmberTools20.[8] The force field other than the partial charges was taken from GAFF2.[9] The force field of chloroform molecule was built in the same way as that of **Ib4**. Before simulating **Ib4** in chloroform, a small box containing 512 chloroform molecules was prepared. The chloroform box was equilibrated for 1 μs at 300K under 1 bar condition. The equilibrated chloroform box was used to solvate **Ib4** in a truncated octahedron by LEaP in AmberTools. The **Ib4** molecule was put at the center of the truncated octahedron, and the minimum distance between the **Ib4** molecule and the boundary was set 15 Å. Then, the simulation system contained the **Ib4** molecule and the 597 chloroform molecules in the truncated octahedron. After energy minimization for the system, MD simulation was performed with periodic boundary condition. The initial velocities of the system were randomly assigned to satisfy Maxwell-Boltzmann distribution at 1 K. The system was heated from 1 K to 298 K for 1 ns and was equilibrated under 1 bar for 1 ns. After that, the production run was done for 1 μs under the canonical condition (the NVT ensemble). The MD simulation was repeated six times. Finally, total 6 μs of six runs were sampled. For high temperatures (348 K and 398 K), additional heating process was conducted for 10 ns before production run. The time step was set to 2 fs throughout the simulations. Non-bonded interactions were evaluated by means of the particle mesh Ewald method with a cutoff of 10 Å.[10] Covalent bonds involving hydrogen atoms were constrained by the SHAKE algorithm.[11] A snapshot was saved every 100 ps. R.M.S.D and dihedral angles from MD trajectories were calculated using cpptraj in AmberTools. 3D molecular images were drawn by UCSF Chimera.[12]

HRMS measurements. Solution of β-peptoids was prepared by dissolving purified compounds in MeCN. All the com-

pounds were measured using positive mode.
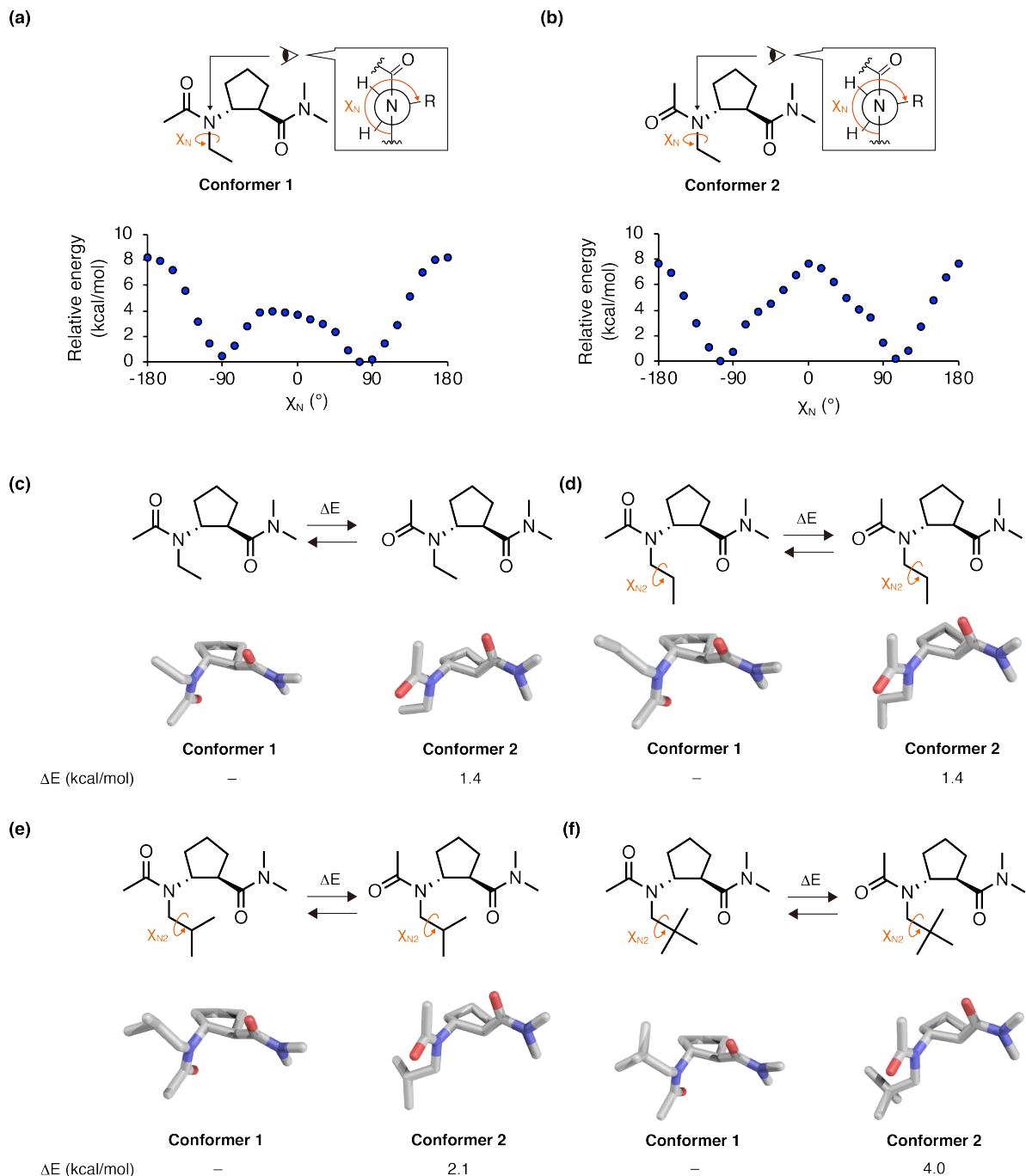
Fig. S1 Structures of ACPC monomers with different *N*-substituents. Geometry optimization of acetyl-*N*-substituted ACPC dimethylamide with ethyl (**Et1**), propyl (**Pr1**), isobutyl (**Ib1**), and neopentyl (**Np1**) group by DFT calculations *in vacuo*. χ_N scan of **(a) conformer 1** and **(b) conformer 2** of **Et1**. Geometry optimized structures of **conformer 1** and **conformer 2** of **(c) Et1**, **(d) Pr1**, **(e) Ib1**, and **(f) Np1**. The difference in energy of the two conformers is shown under each structure.

Ibu2

Conformer 1		Conformer 2
ΔE (kcal/mol)	–	4.3 kcal/mol

Residue	ω	φ	θ	ψ
1	177.6°	−62.7°	−79.7°	156.6°
2	176.6°	−63.9°	−82.1°	162.1°

Residue	ω	φ	θ	ψ
1	19.5°	103.2°	−69.8°	126.6°
2	19.1°	104.6°	−97.8°	161.2°

Ibu3

Conformer 1		Conformer 2
ΔE (kcal/mol)	–	6.7 kcal/mol

Residue	ω	φ	θ	ψ
1	177.6°	−62.8°	−79.2°	156.2°
2	180.0°	−63.9°	−80.4°	160.3°
3	176.5°	−63.7°	−81.9°	162.5°

Residue	ω	φ	θ	ψ
1	19.1°	104.6°	−68.4°	130.6°
2	26.3°	111.1°	−69.8°	128.2°
3	18.9°	104.9°	−98.3°	161.9°

Ibu4

Conformer 1		Conformer 2
ΔE (kcal/mol)	–	9.1 kcal/mol

Residue	ω	φ	θ	ψ
1	177.7°	−62.9°	−79.3°	156.4°
2	180.0°	−63.9°	−79.7°	160.0°
3	179.7°	−63.5°	−80.0°	160.6°
4	176.3°	−63.7°	−82.1°	162.5°

Residue	ω	φ	θ	ψ
1	18.8°	104.5°	−68.7°	129.2°
2	24.1°	112.1°	−68.9°	132.9°
3	25.4°	111.9°	−69.8°	128.4°
4	19.3°	104.8°	−98.4°	161.5°

Fig. S2 Conformations of ACPC oligomers optimized with DFT calculations. Conformations of **Ib2**, **Ib3** and **Ib4** with trans amide (**conformer 1**) and cis amide (**conformer 2**). The difference in energy of the two conformers of each oligomer is shown under each structure.
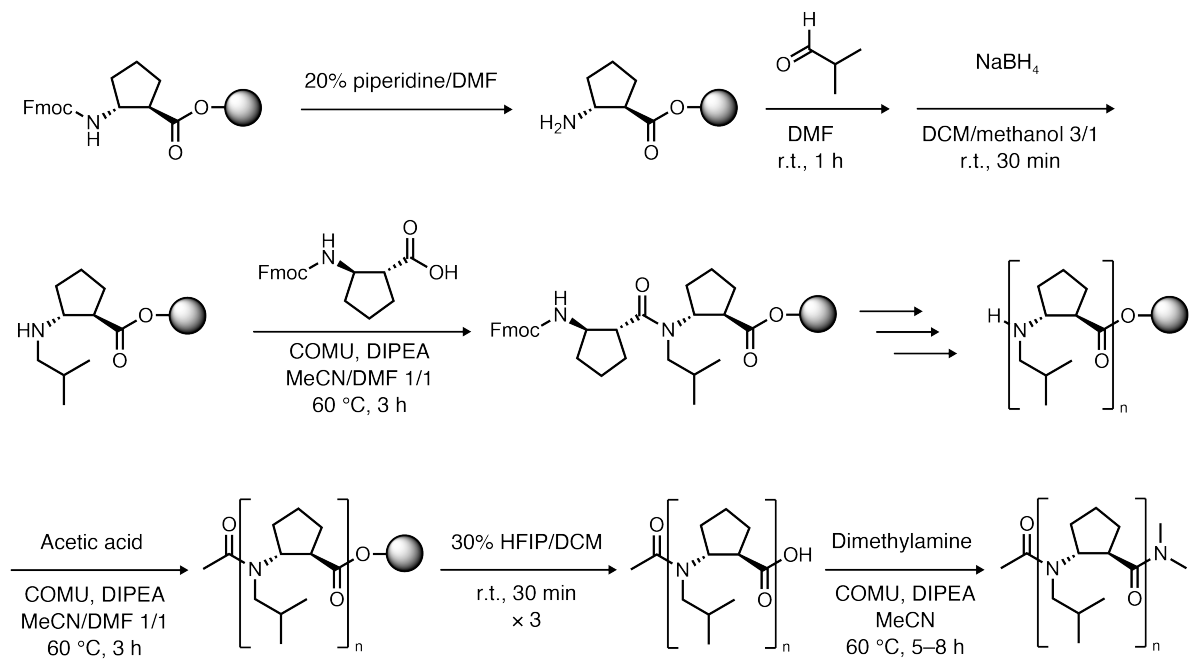
Scheme S1. Solid phase synthesis of *N*-isobutyl-ACPC oligomers.
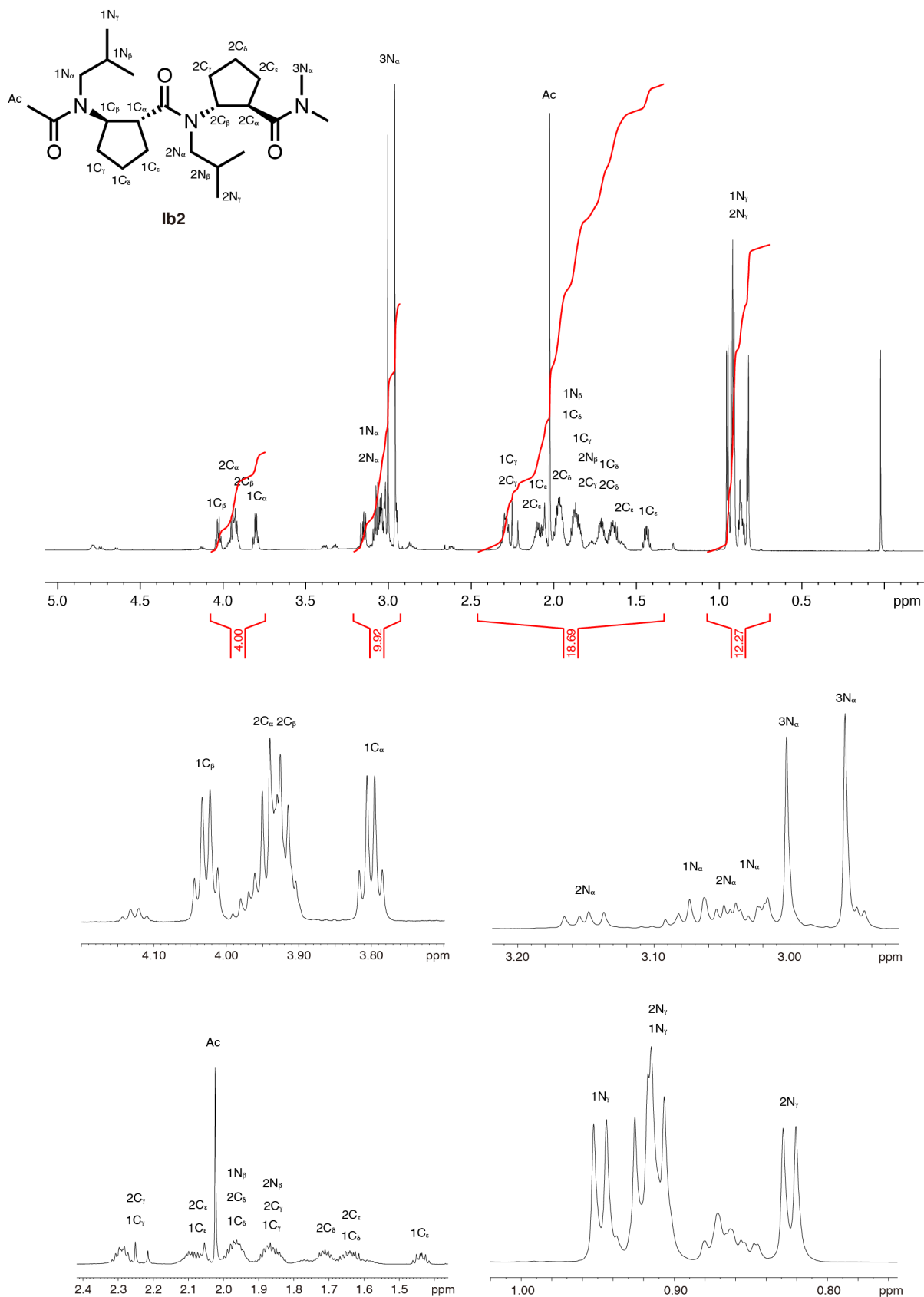
Fig. S3 ¹H NMR spectrum of Ib2. The spectrum was recorded in CDCl₃ at 25 °C. Close-up views of the spectrum are shown under the full spectrum.
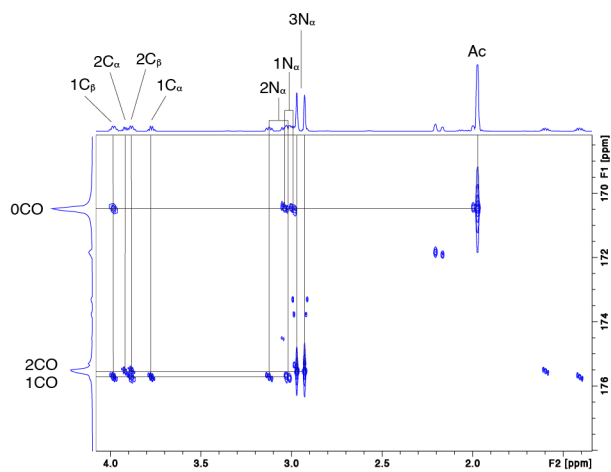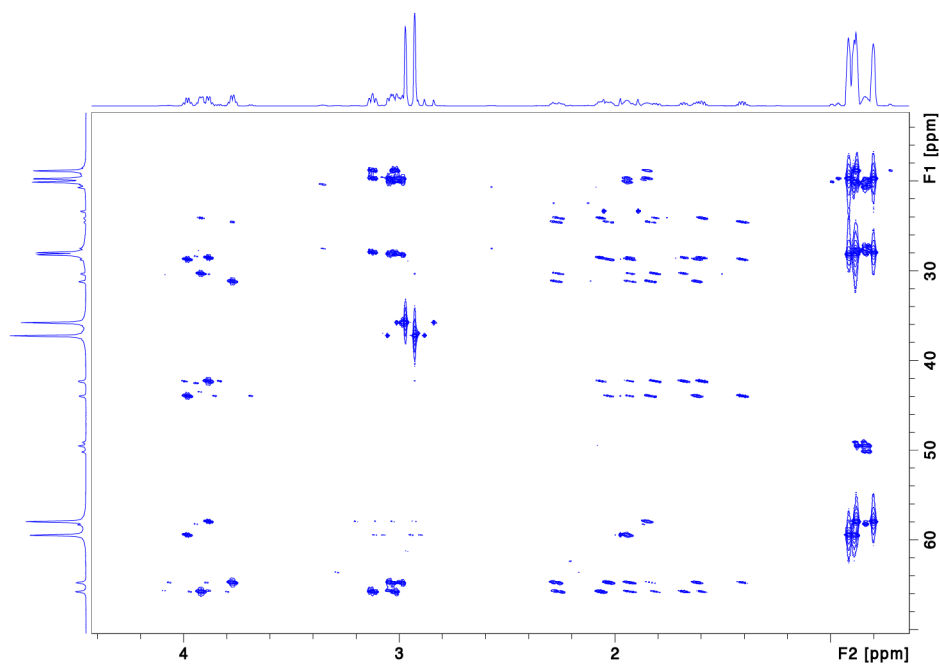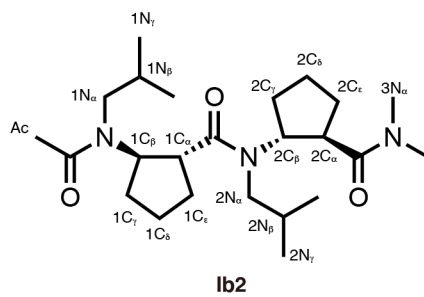
Fig. S4 HMBC spectrum of Ib2. The spectrum was recorded in CDCl₃ at 25 °C. Aliphatic-aliphatic and carbonyl-aliphatic regions of the spectrum are shown as the top and bottom panels, respectively.
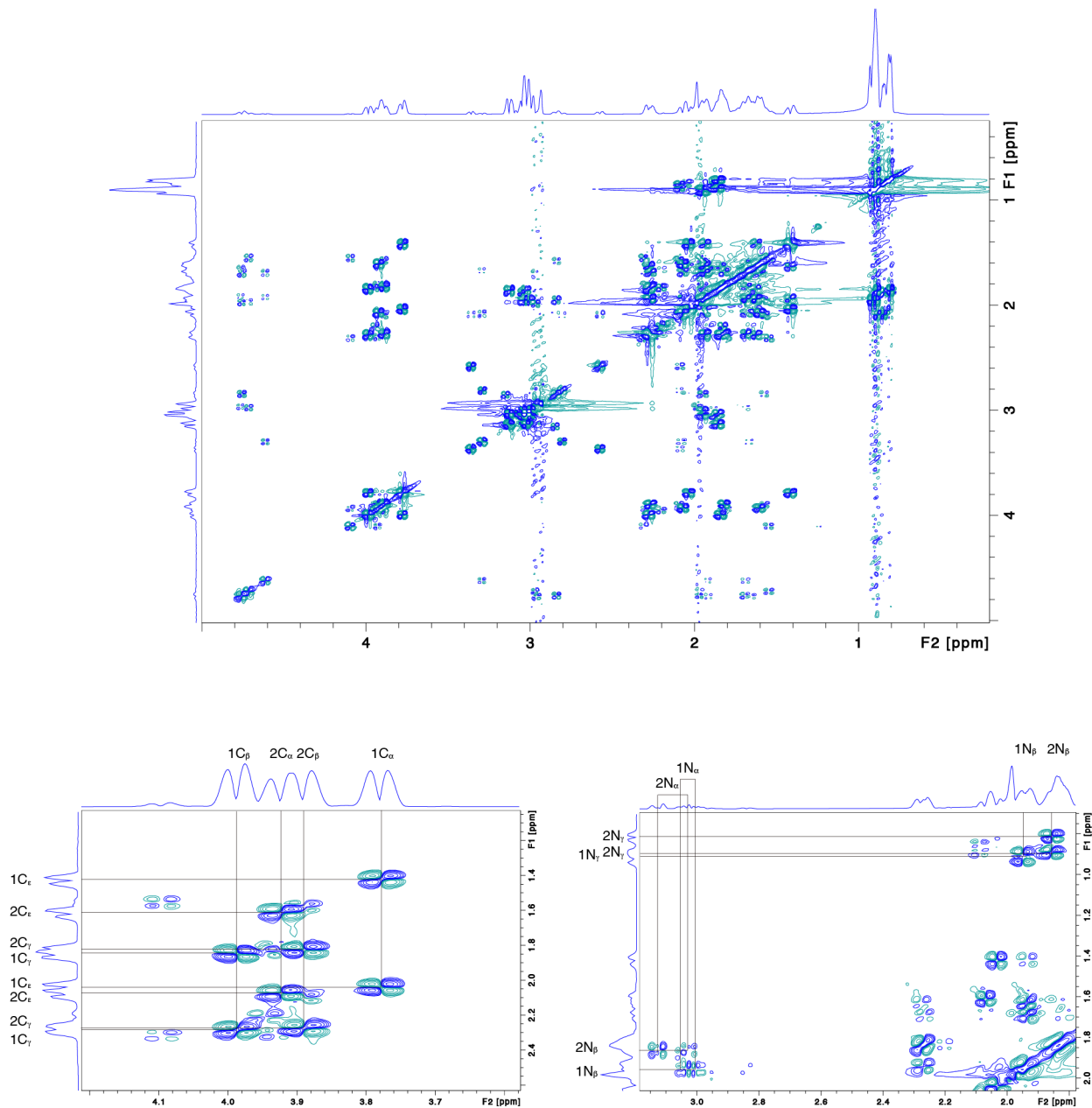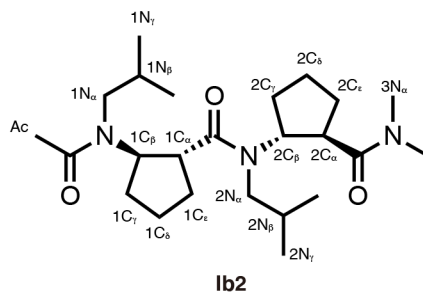
Fig. S5 COSY spectrum of Ib2. The spectrum was recorded in CDCl₃ at 25 °C. Close-up views of the spectrum are shown under the full spectrum.
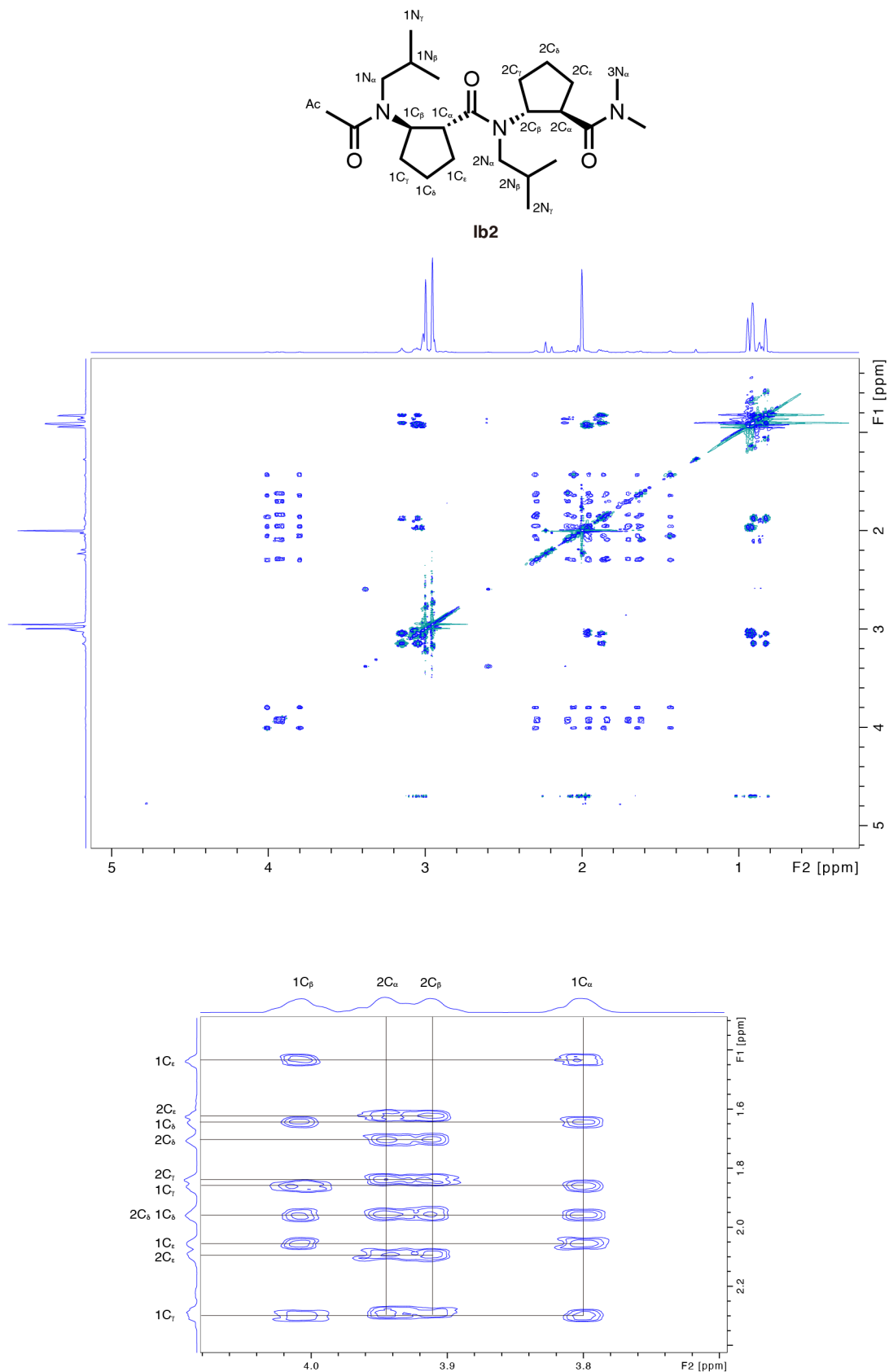
Fig. S6 TOCSY spectrum of Ib2. The spectrum was recorded in CDCl₃ at 25 °C. A close-up view of the spectrum is shown under the full spectrum.
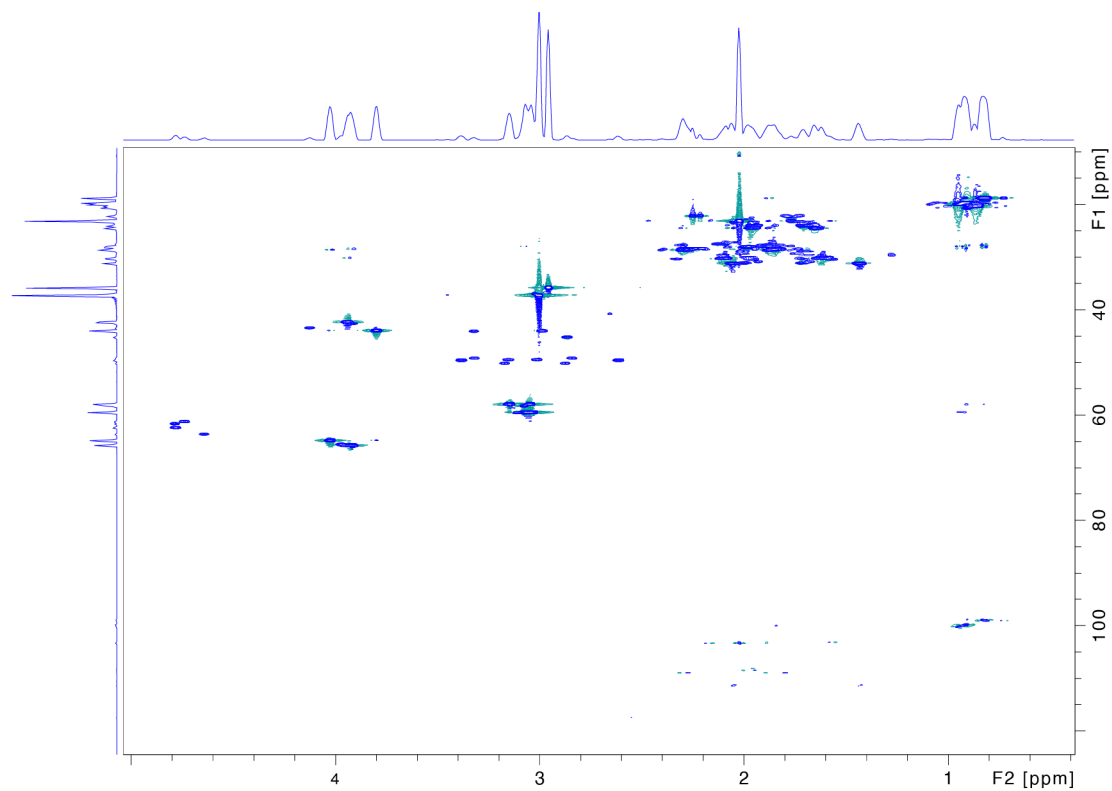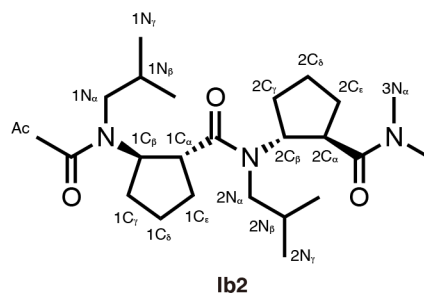
Fig. S7 HSQC spectrum of Ib2. The spectrum was recorded in CDCl₃ at 25 °C.

Table S1. Chemical shifts of protons and carbons of Ib2 observed on the NMR spectra.

Ib2
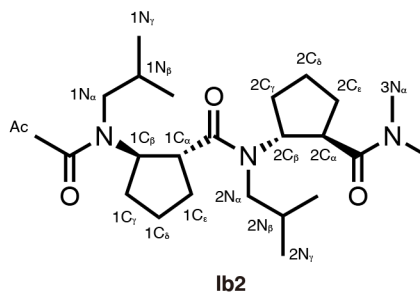
(ppm)

	Major conformer (trans-trans)		Minor conformer (trans-cis)		Minor conformer (cis-trans)		Minor conformer (cis-cis)	
	^{1}H	^{13}C	^{1}H	^{13}C	^{1}H	^{13}C	^{1}H	^{13}C
Ac	2.02	23.2	2.02	23.2	2.25	22.2	2.21	22.2
0CO		170.5		170.4		171.8		171.9
1C$_\alpha$	3.80	44.0	4.13	43.5	2.87	45.2	3.32	44.1
1C$_\beta$	4.03	64.8	3.96	65.6	4.78	62.5	4.64	63.7
1C$_\gamma$	1.87 2.30	28.6						
1C$_\delta$	1.65 1.96	24.6						
1C$_\varepsilon$	1.44 2.06	31.2						
1N$_\alpha$	3.04 3.07	59.5	3.06 3.15	59.5	2.62 3.38	49.6	2.84 3.32	49.3
1N$_\beta$	1.98	28.2						
1N$_\gamma$	0.92 0.94	19.7 20.0						
1CO		175.7		176.7		174.5		175.8
2C$_\alpha$	3.94	42.4	2.99	44.0	3.91	42.5	4.03	44.0
2C$_\beta$	3.92	65.8	4.74	61.3	3.96	65.6	4.79	61.7
2C$_\gamma$	1.87 2.30	28.6						
2C$_\delta$	1.71 1.96	24.1						
2C$_\varepsilon$	1.62 2.09	30.3						
2N$_\alpha$	3.05 3.15	57.9	3.01 3.15	49.5	3.08	58.3	2.87 3.17	50.3
2N$_\beta$	1.88	28.0						
2N$_\gamma$	0.83 0.91	18.8 19.7						
2CO		175.5		173.3		175.5		173.8
3N$_\alpha$	2.96 3.00	35.8 37.3						

The information of trans/cis configurations of each amide bond of the conformer is shown in parentheses on the top of the table. For the minor conformers, only the backbone protons and carbons (Ac, C$_\alpha$, C$_\beta$, CO, and N$_\alpha$ protons and carbons) were assigned.
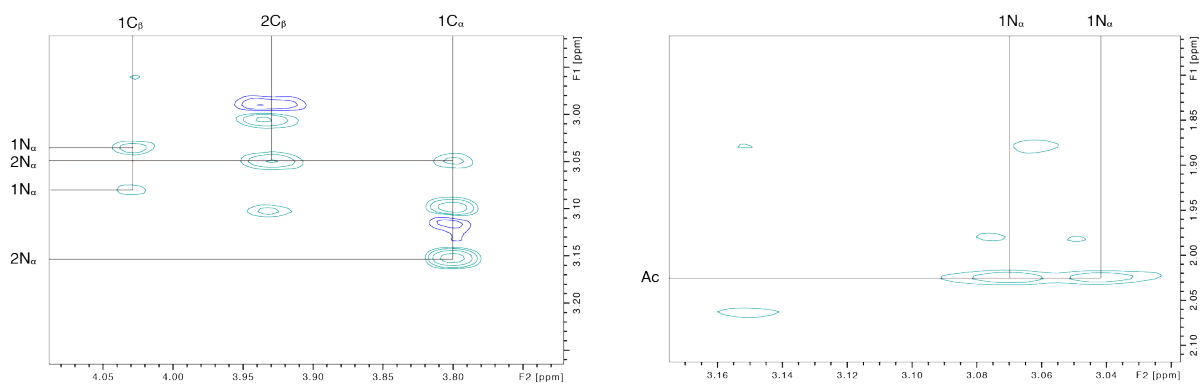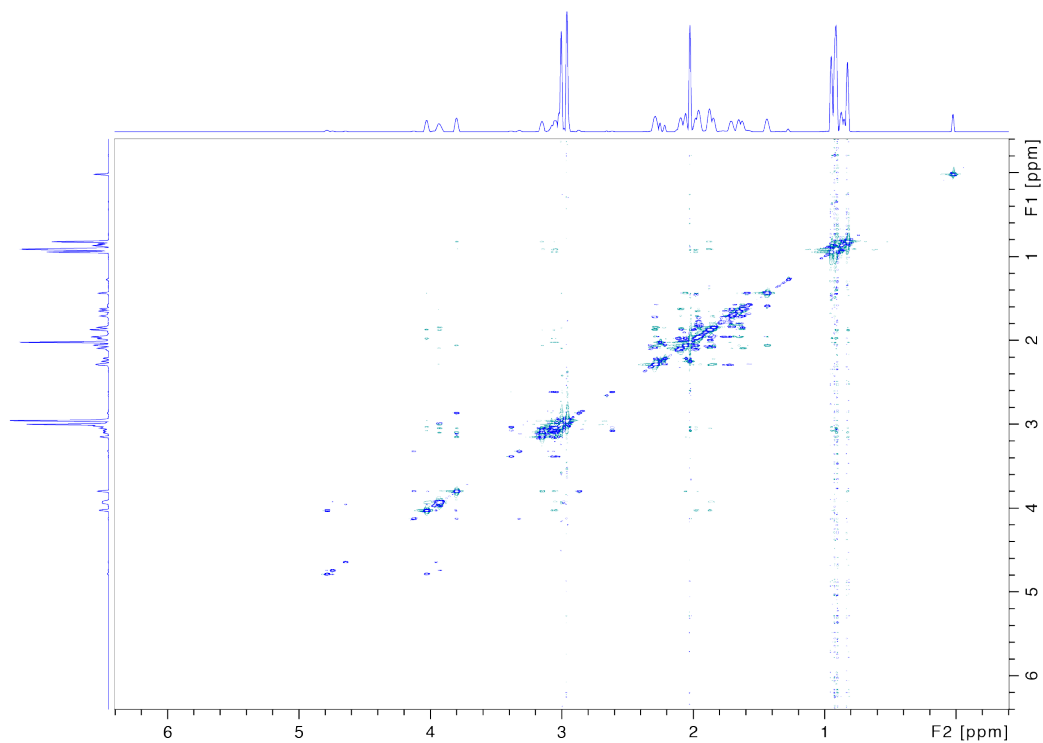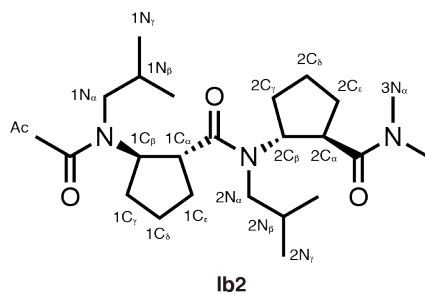
Fig. S8 A 2D gradient-selected F1-PSYCHE-EASY-ROESY spectrum of Ib2. The spectrum was recorded in CDCl₃ at 25 °C. Closeup views of the spectrum are shown under the full spectrum. NOEs supporting the rotational restrictions around ϕ, ψ and ω angles are indicated with black lines.
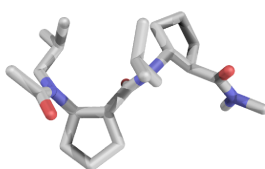
Ib2 in chloroform

Residue	ω	φ	θ	ψ
1	−175.3°	−62.6°	−86.2°	145.8°
2	176.2°	−63.9°	−86.6°	165.5°

Fig. S9 Geometry optimized structure of Ib2 in chloroform. The backbone dihedral angles of the structure are shown in the table at the bottom.
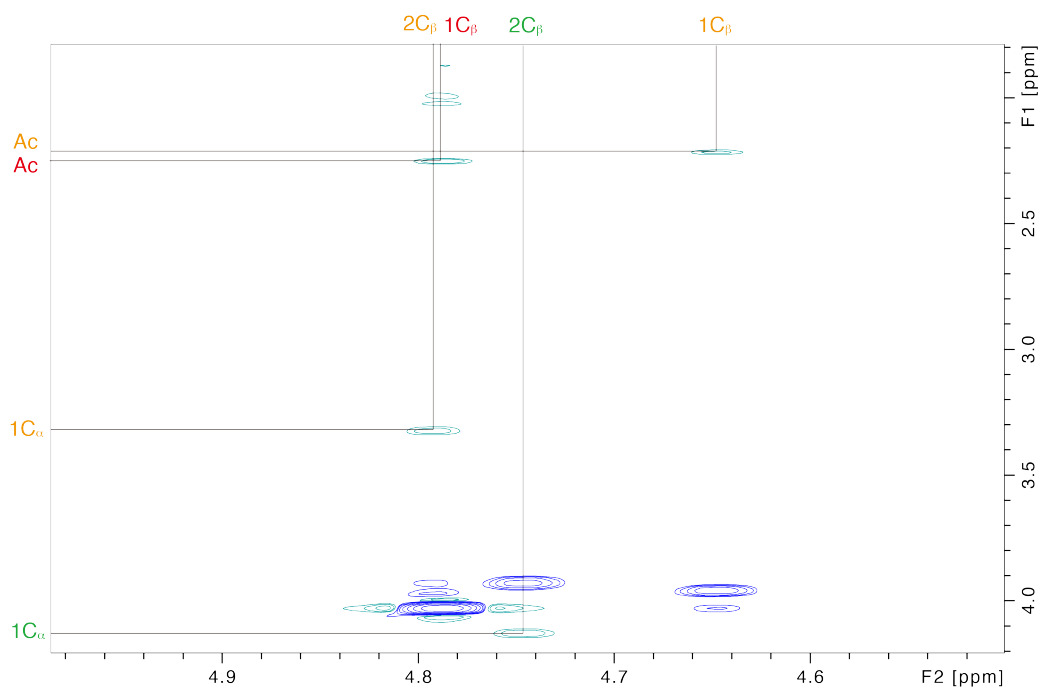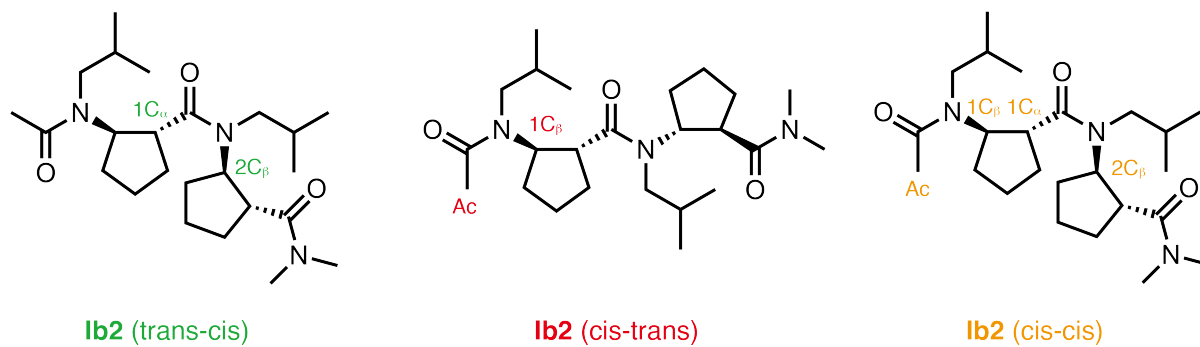
Fig. S10 NOEs indicating the cis amides in minor conformers of Ib2. An enlarged view of an EASY-ROESY spectrum of **Ib2** where the NOEs indicating the cis amides in minor conformers appear. The atom names are indicated with the color corresponding to the conformer structure shown above the spectrum.
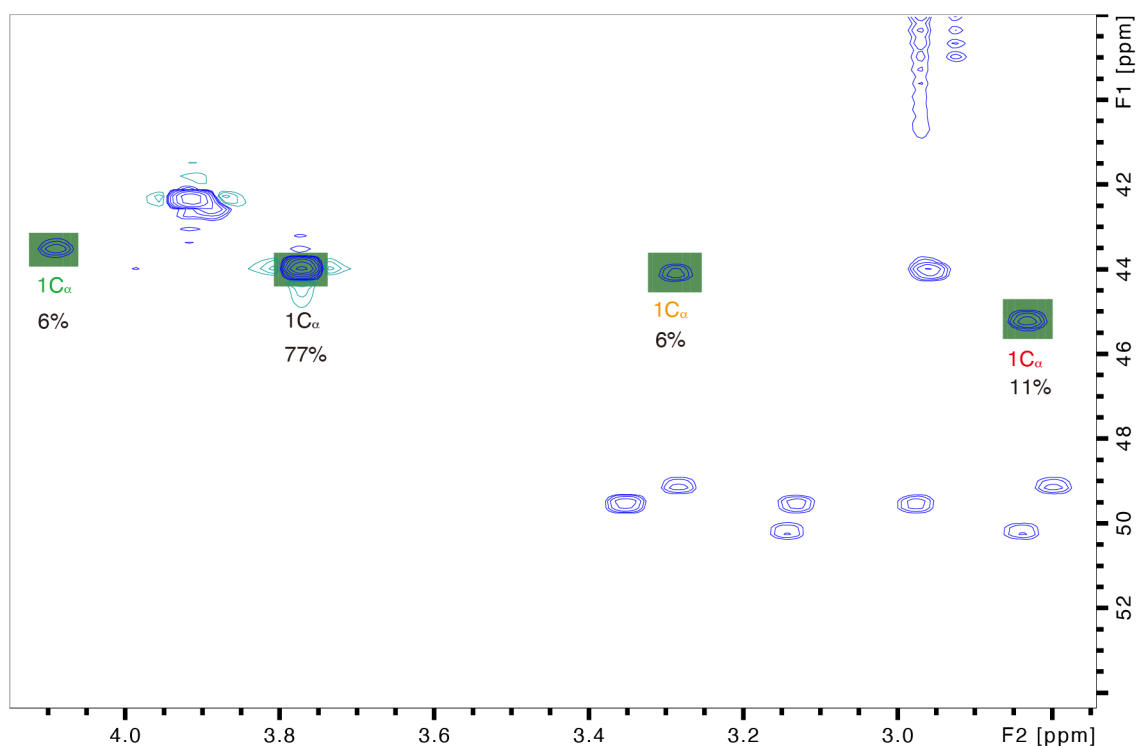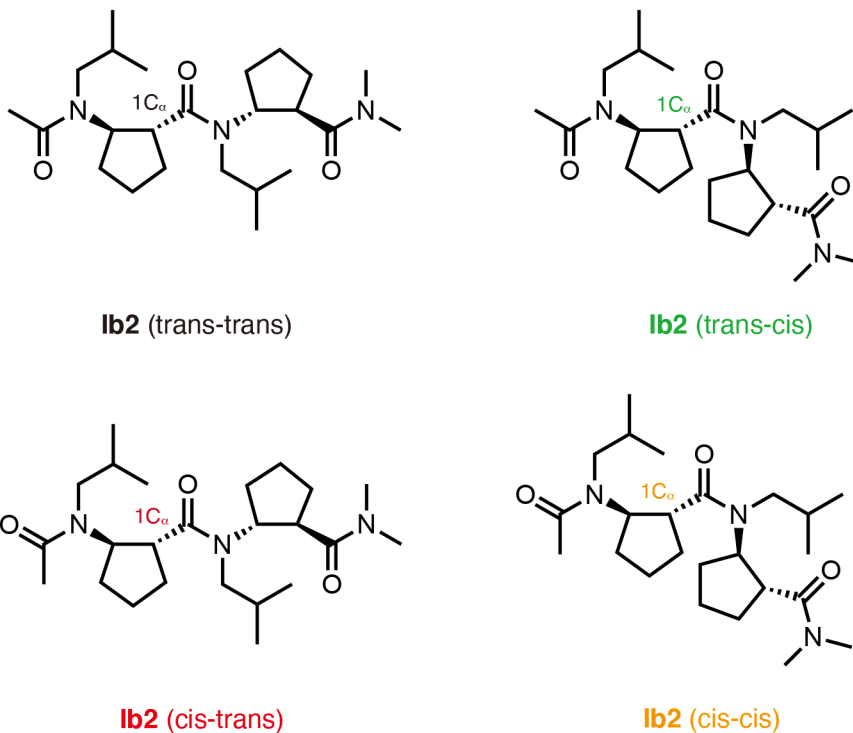
Fig. S11 HSQC cross peaks used for determining the populations of minor conformers. An enlarged view of the HSQC spectrum of **Ib2** where the cross peaks indicating the $1C_\alpha$ are shown. The ratio of each cross peak area is shown under the peak. The $1C_\alpha$ proton was chosen for determining the conformer ratio because the peak was assigned for all the conformers and all the peaks are not overlapping with other peaks.

(a) 298 K

| Run 2 | Run 3 | Run 4 | Run 5 | Run 6 |

(b) 348 K

| Run 2 | Run 3 | Run 4 | Run 5 | Run 6 |

(c) 398 K

| Run 2 | Run 3 | Run 4 | Run 5 | Run 6 |
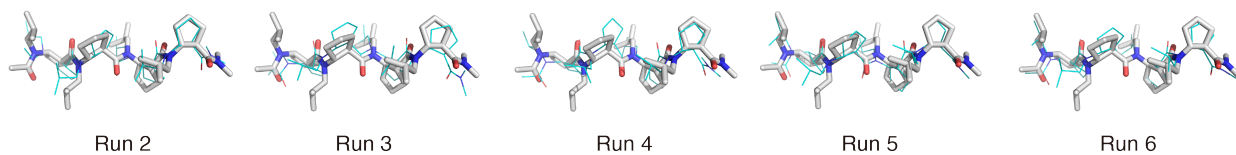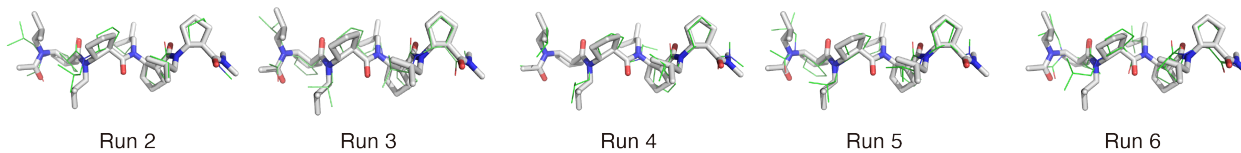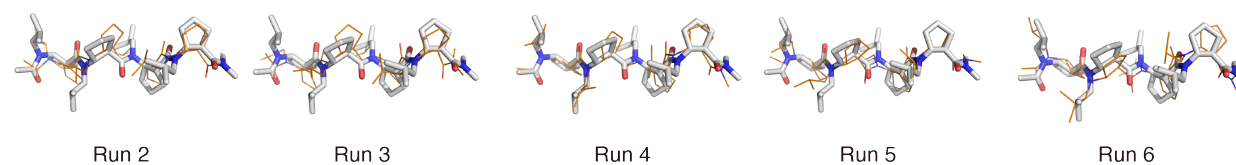
Fig. S12 Conformations of Ib4 before and after 1 μs MD simulations. Conformations before (gray) and after 1 μs MD simulations at 298 K (blue), 348 K (green), and 398 K (orange).
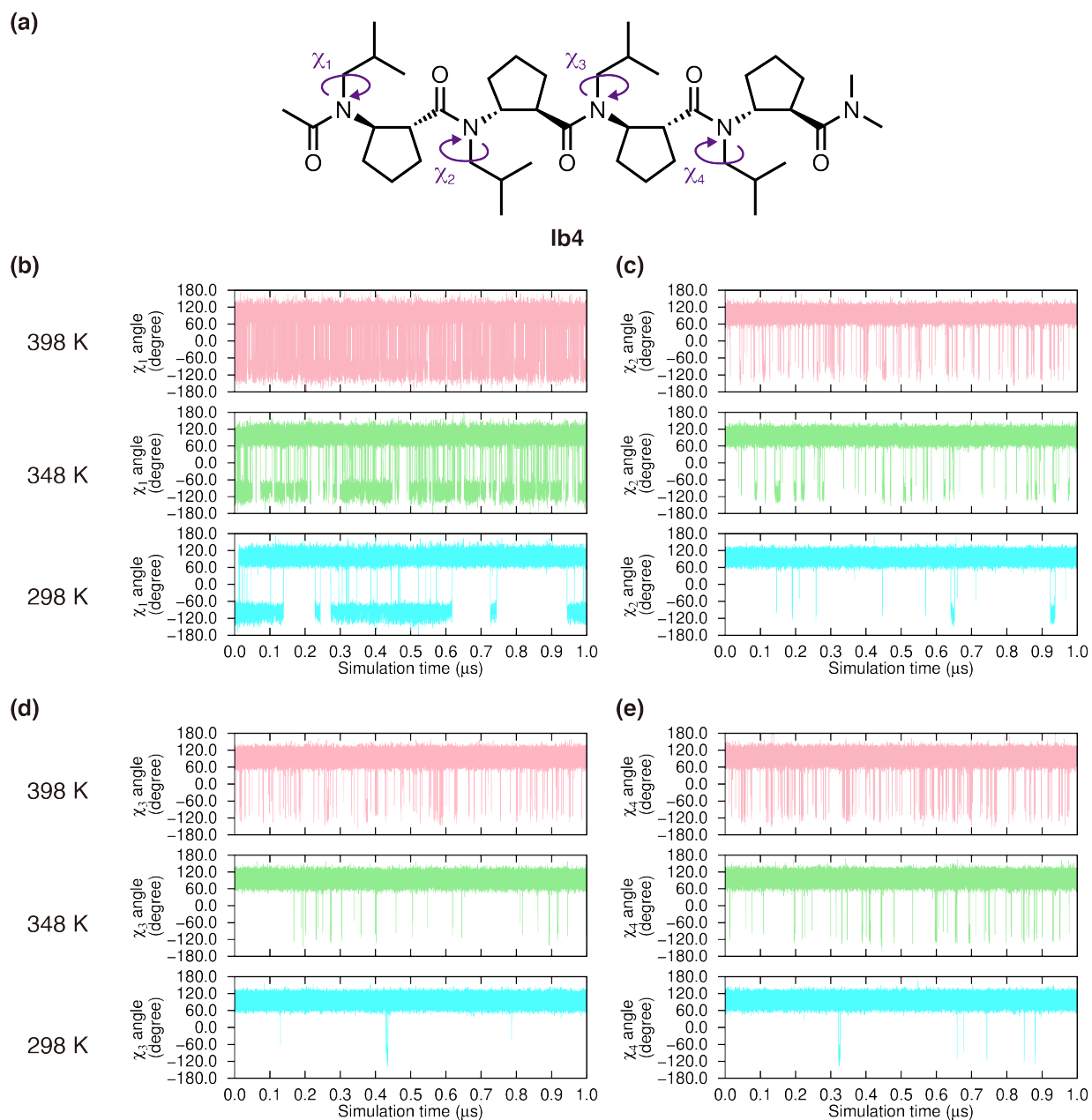
Fig. S13 Dihedral χ$_N$ angle rotation during MD simulation. The dihedral angles χ$_1$, χ$_2$, χ$_3$ and χ$_4$ of **Ib4** were described in the panel **(a)**. The time plots of the dihedral angles **(b)** χ$_1$, **(c)** χ$_2$, **(d)** χ$_3$ and **(e)** χ$_4$ were drawn as the lines at 298 K (light-blue), 348 K (light-green) and 398 K (light-pink). The lines derived from the six MD runs were overlaid.

(a)

Ib2

(b)

Ib4
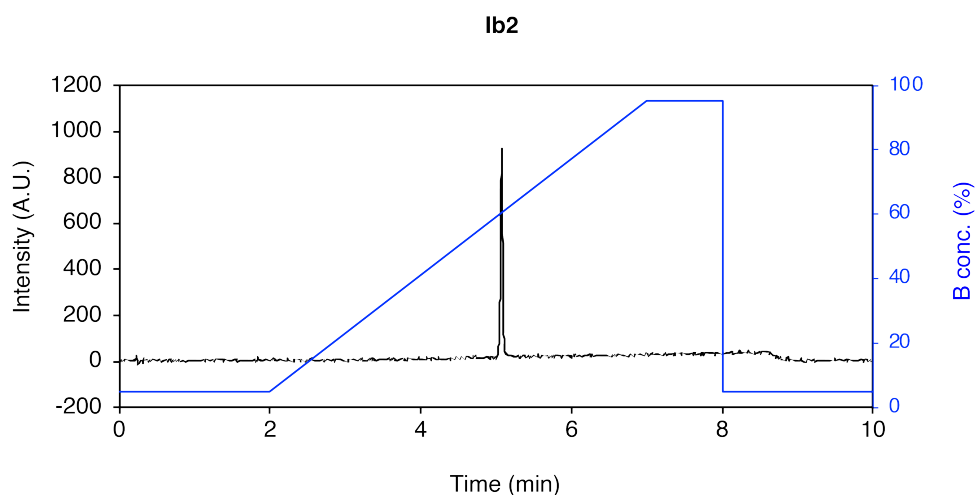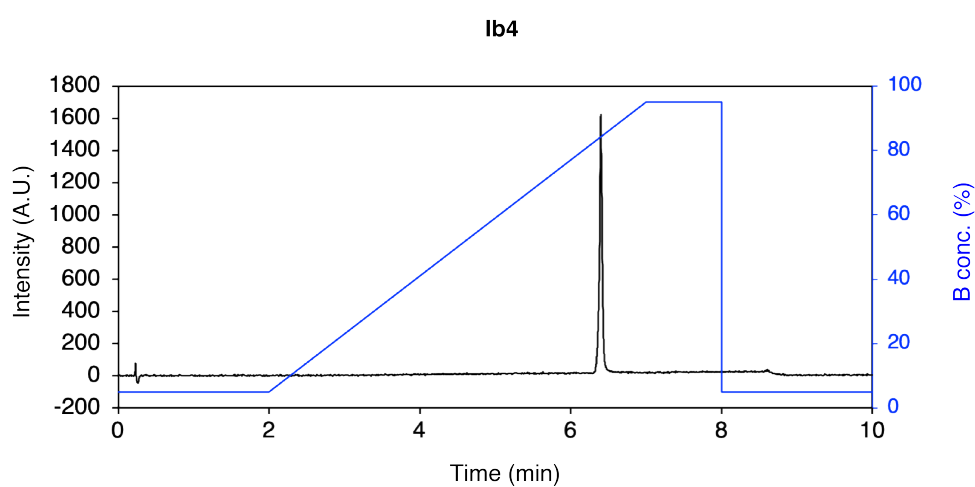
Fig. S14 UPLC chromatograms of (a) Ib2 and (b) Ib4 after HPLC purification. The analysis was conducted on a UPLC system using water containing 0.01% formic acid (solvent A) and MeCN containing 0.01% formic acid (solvent B). The gradient programs of solvent B are indicated using blue lines on the chromatograms. The column was heated at 60 °C during the analysis. The elution was monitored with the absorbance at 220 nm.

References

1   M. D. Hanwell, D. E. Curtis, D. C. Lonie, T. Vandermeersch, E. Zurek and G. R. Hutchison, *J. Cheminform.*, 2012, **4**, 1–17.

2   M. J. Frisch, G. W. Trucks, H. B. Schlegel, G. E. Scuseria, M. A. Robb, J. R. Cheeseman, G. Scalmani, V. Barone, G. A. Petersson, H. Nakatsuji, X. Li, M. Caricato, A. V. Marenich, J. Bloino, B. G. Janesko, R. Gomperts, B. Mennucci, H. P. Hratchian, J. V. Ortiz, A. F. Izmaylov, J. L. Sonnenberg, D. Williams-Young, F. Ding, F. Lipparini, F. Egidi, J. Goings, B. Peng, A. Petrone, T. Henderson, D. Ranasinghe, V. G. Zakrzewski, J. Gao, N. Rega, G. Zheng, W. Liang, M. Hada, M. Ehara, K. Toyota, R. Fukuda, J. Hasegawa, M. Ishida, T. Nakajima, Y. Honda, O. Kitao, H. Nakai, T. Vreven, K. Throssell, J. Montgomery, J. A., J. E. Peralta, F. Ogliaro, M. J. Bearpark, J. J. Heyd, E. N. Brothers, K. N. Kudin, V. N. Staroverov, T. A. Keith, R. Kobayashi, J. Normand, K. Raghavachari, A. P. Rendell, J. C. Burant, S. S. Iyengar, J. Tomasi, M. Cossi, J. M. Millam, M. Klene, C. Adamo, R. Cammi, J. W. Ochterski, R. L. Martin, K. Morokuma, O. Farkas, J. B. Foresman and D. J. Fox, .

3   P. R. LePlae, N. Umezawa, H. S. Lee and S. H. Gellman, *J. Org. Chem.*, 2001, **66**, 5629–5632.

4   J. Ilgen, J. Nowag, L. Kaltschnee, V. Schmidts and C. M. Thiele, *J. Magn. Reson.*, 2021, **324**, 106900.

5   C. M. Thiele, K. Petzold and J. Schleucher, *Chem. - A Eur. J.*, 2009, **15**, 585–588.

6   D. A. Case, K. Belfon, I. Y. Ben-Shalom, S. R. Brozell, D. S. Cerutti, T. E. I. Cheatham, V. W. D. Cruzeiro, T. A. Darden, R. E. Duke, G. Giambasu, M. K. Gilson, H. Gohlke, A. W. Goetz, R. Harris, S. Izadi, S. A. Izmailov, K. Kasavajhala, A. Kovalenko, R. Krasny, T. Kurtzman, T. S. Lee, S. LeGrand, P. Li, C. Lin, J. Liu, T. Luchko, R. Luo, V. Man, K. M. Merz, Y. Miao, O. Mikhailovskii, G. Monard, H. Nguyen, A. Onufriev, F. Pan, S. Pantano, R. Qi, D. R. Roe, A. Roitberg, C. Sagui, S. Schott-Verdugo, J. Shen, C. L. Simmerling, N. R. Skrynnikov, J. Smith, J. Swails, R. C. Walker, J. Wang, L. Wilson, R. M. Wolf, X. Wu, Y. Xiong, Y. Xue, D. M. York and P. A. Kollman, *AMBER 2020, Univ. California, San Fr.*

7   G. M. J. Barca, C. Bertoni, L. Carrington, D. Datta, N. De Silva, J. E. Deustua, D. G. Fedorov, J. R. Gour, A. O. Gunina, E. Guidez, T. Harville, S. Irle, J. Ivanic, K. Kowalski, S. S. Leang, H. Li, W. Li, J. J. Lutz, I. Magoulas, J. Mato, V. Mironov, H. Nakata, B. Q. Pham, P. Piecuch, D. Poole, S. R. Pruitt, A. P. Rendell, L. B. Roskop, K. Ruedenberg, T. Sattasathuchana, M. W. Schmidt, J. Shen, L. Slipchenko, M. Sosonkina, V. Sundriyal, A. Tiwari, J. L. Galvez Vallejo, B. Westheimer, M. Włoch, P. Xu, F. Zahariev and M. S. Gordon, *J. Chem. Phys.*, 2020, **152**, 154102.

8   J. Wang, W. Wang, P. A. Kollman and D. A. Case, *J. Mol. Graph. Model.*, 2006, **25**, 247–260.

9   X. He, V. H. Man, W. Yang, T. S. Lee and J. Wang, *J. Chem. Phys.*, 2020, **153**, 114502.

10   T. Darden, D. York and L. Pedersen, *J. Chem. Phys.*, 1993, **98**, 10089–10092.

11   J. P. Ryckaert, G. Ciccotti and H. J. C. Berendsen, *J. Comput. Phys.*, 1977, **23**, 327–341.

12   E. F. Pettersen, T. D. Goddard, C. C. Huang, G. S. Couch, D. M. Greenblatt, E. C. Meng and T. E. Ferrin, *J. Comput. Chem.*, 2004, **25**, 1605–1612.